Supplemental Information

Chiral Meso-structured Hydroxyapatite on 3D Macroporous Coralline Scaffolds for Selective Osteogenesis

Chao Zhou[a†], Anqi Liu[b†], Ping Li[c†], Jing Ai[d], Lu Han[d], Shaoyang Zhang[c], Shuai Chen[a], Ouyang Yuanming[a*], baojie Li[c*], Shunai Che[e*]and Cunyi Fan[a*]

a. Department of Orthopaedics, Shanghai Engineering Research Center for Orthopaedic Material Innovation and Tissue Regeneration, Shanghai Sixth People's Hospital Affiliated to Shanghai Jiao Tong University School of Medicine, 600 Yishan Road, Shanghai 200233, China.

b. Department of Orthodontics, Shanghai Stomatological Hospital & School of Stomatology, Fudan University, Beijing East Road No.356,   Shanghai 200001, China. Huangpu District. Shanghai Key Laboratory of Craniomaxillofacial Development and Diseases, Fudan University, Tianjin Road No.2, Huangpu District, Shanghai 200001, China.

c. Bio-X Center, Key Laboratory for the Genetics of Developmental and Neuropsychiatric Disorders, Ministry of Education, Shanghai Jiao Tong University, 800 Dongchuan Road, Shanghai, 200240, China.

d. School of Chemical Science and Engineering, Tongji University, 1239 Siping Road, Shanghai, 200092, China.

e. School of Chemistry and Chemical Engineering, State Key Laboratory of Composite Materials, Frontiers Science Center for Transformative Molecules, Shanghai Key Laboratory for Molecular Engineering of Chiral Drugs, Shanghai Jiao Tong University, 800 Dongchuan Road, Shanghai, 200240, China.

E-mail: ouyangyuanming@163.com, libj@sjtu.edu.cn; chesa@sjtu.edu.cn, cyfan@sjtu.edu.cn

[†]   These   authors   contributed   equally   to   this   work.

This PDF file includes:

Supplementary Figures and Legends and methods.

MATERIALS AND METHODS

Materials

Diammonium hydrogen phosphate ($NH_4H_2PO_4$; 99.8%), Urea (98%), were purchased from Sinopharm Chemical Reagent Co., Ltd. D-, L- and Racemic-tartaric acid (99.9%) was obtained from Tansoole Co., Ltd. Nitric acid (99.9%), amino acids were obtained from J & K Chemical Technology. Corallite was obtained from Tmall, china. All of the reagents were used as received without further purification. All water used was ultrapure (18.2 MΩ/cm), obtained from a Heal Force SMART Ultra-pure water system.

Substrate treatment

The coral stone is soaked in a large amount of deionized water, then washed with water and ethanol for three times alternately under ultrasonic environment, and finally dried for standby. Then, it was processed into 2g sized particles and ultrasonic cleaning and drying.

Preparation of CMHAP@CL

The preparation of CMHAP@CL with well-controlled chiral structure was carried out by our previously reported methods of synthesize chiral inorganic materials[42-46]. In a typical procedure, 1 mmol diammonium hydrogen phosphate and 2.23 mmol urea were dissolved in 20 mL H_2O denote as A. 1 mmol D-, or L-, or Racemic tartaric acid was dissolved in 10 mL H_2O denote as B. Corallite denote as C. Then, 2g C was quickly added in B, subsequently A was added in BC mixed solution under vigorous magnetic stirring. RT keep stir 10 min. After that, take out the magneton and transfer to the autoclave, the container was then closed and maintained at 180 ℃ for 2-24 h. After that, the autoclave was cooled to room temperature naturally. Use deionized water and ethyl alcohol washing several times make sure that any remaining organic molecules are removed and dried in vacuum drying oven under 60 ℃ overnight.

Structure and performance characterization of the CMHAP@CL

X-Ray Powder Diffraction (XRD)

XRD patterns were recorded on a Rigaku X-ray diffractometer D/MAX–2200/PC equipped with Cu Kα radiation (40 kV, 30 mA, λ = 0.15418 nm), at the rate of 1 ° min-1 over the range 10-80 °.

Scanning electron microscopy (SEM)

The macroscopic features of the samples were observed with SEM (JEOL JSM-7900F) with an accelerating voltage of 1.0 kV and working distance at 4 mm to minimize charge accumulation.

Transmission electron microscopy (TEM)

TEM experiment was performed using a JEOL JEM-F200 microscope that equipped with a Schottky gun operating at 200 kV (Cs 1.0 mm, Cc 1.1 mm, point resolution of 1.9 Å for TEM). Images were recorded using GATAN OneView IS camera (4096 × 4096 pixels) under low-dose conditions.

X-ray microscopy (XRM)

To three-dimensionally reconstruct the CMHAP@CL, we scanned the CL and CMHAP@CL at the micro-CT laboratory of Instrument Analysis Center, using a 3D X-ray microscope (3D-XRM), Zeiss

Xradia 520 versa. Unlike conventional micro-CT, which relies on maximum geometric magnification and a flat panel detector to achieve high resolution, 3D-XRM uses CCD-based objectives to achieve higher spatial resolution. Based on the size of the CMHAP@CL specimen, a CCD-based 0.4× objective was used, providing isotropic voxel sizes of 6.587 μm with the help of geometric magnification. During the scan, the acceleration voltage for the X-ray source was 60 kV (current 83μA), and a thin filter (LE1) was used to avoid beam-hardening artifacts. To improve signal-to-noise ratio, 2001 projections over 360° were collected, and the exposure time for each projection was 2s. Volume data processing was performed using software VG Studio Max (version 3.0; Volume Graphics). The ORS Dragonfly (ORS version 4.0) was used to reconstruct the spatial arrangement of the CMHAP@CL.

Micro-CT

Bone formation was evaluated by a scanco μ-CT50 scanner for specimens of the material after osteogenesis using X-ray voltage of 60 kV, current of 500 μA, effective pixel size of 9 μm. A 3D reconstruction was accomplished by NRecon (Skyscan, Kontich, Belgium) software. The bone volume fraction of the defect sites were calculated by Heidelberg-mCT-Analyzer software.

Circular dichroism spectrometer(CD)

DRCD and UV/Vis spectra were obtained using a JASCO J-815 spectropolarimeter fitted with a DRCD apparatus. The scaffold was placed between the normally incident light and a black backboard. All of the reflected light was collected by an integrating sphere before reaching the CD detector.

Scaffolds pretreatment and implantation

Scaffolds pretreatment: 1) all the scaffolds were heat sterilized; 2) soaking the scaffolds in α-MEM (Thermo Fisher) and then implantation.

Implantation of the Scaffolds in Nude Mice

Two-month-old nude mice were kept in controlled environment, cared for and treated regarding to the institutional guidelines (The ethic approval no. [SYXK (SH) 2011-0112], Institutional Animal Care and Use Committee of Shanghai). The animals were anesthetized intramuscularly by the mixture of Xylazine (25 mg/ml), Ketamine (25 mg/ml), and Zoletil (12.5 mg/ml) at 1:1:1 volume ratio with a 100 μl volume per 25 g body weight. The scaffolds were implanted on the back of the mice. The experiment was performed on triplicate mice, each carrying the duplicate of three sample types: Ach-MHAP@CL, L-CMHAP@CL and D-CMHAP@CL (Figure 3a). Control scaffolds, called Ach-MHAP@CL, were prepared by adding no chiral molecule. They were manipulated using similar manners as described for the tested scaffolds. The animals were euthanized 12 and 24 weeks after implantation. The grafts were then removed and processed for histological analysis and mCT-scanned. To quantify the bone-like tissues, 10 images of each sample were taken randomly to measure the area of new bone formation versus total area.

Histological Analysis

The implanted grafts were fixed overnight in 4% PBS-buffered paraformaldehyde overnight at 4°C. The samples were then stored in 70% alcohol for further experiments. For paraffin sections, samples were decalcified in 15% EDTA for 2-4 weeks and then dehydrated in alcohol, cleared with xylene,

and embedded in paraffin. Five-mm-thick sections were cut using microtome (Lexica Microsystems Nussle GmbH). Hematoxylin-eosin (HE) staining was carried out on bone sections. Stained slides were photographed under a light microscope (Lexica).For each sample, at least two different section levels and two histological sections for each level were analyzed.

Immunohistochemical staining

For immunohistochemical staining, endogenous peroxidase activity was quenched with 3% H_2O_2 in methanol for 20 mins followed by washing with PBS before primary antibody incubation. After incubation with secondary antibody, sections were developed with diaminobenzidine and counter-stained with hematoxylin and then dehydrated and mounted in neutral resins. Primary antibodies were: OCN, OPN, RUNX2, Non-immune immunoglobulin G (IgG) (of the same species as the primary antibodies) was used as negative controls.

Total RNA extraction and quantitative polymerase chain reaction (qPCR)

Total RNA was extracted using TRIzol (Invitrogen), and 1 μg total RNA was used to synthesize complementary DNA using a reverse transcription kit (Takara). For quantitative PCR, SYBR Green PCR Master Mix (Applied Biosystems) was used in a CFX96 Real-Time System thermocycler (Bio-Rad); the RNA levels of the target genes were normalized to those of Gapdh. For each qPCR experiment, all samples were run in triplicate. Primer sequences are listed in the chemicals. All gene expression fold changes were normalized to the Ach-MHAP@CL group.

Statistical analysis

The data are presented as the mean ± SD and were analysed by two-tailed Student's t-tests (GraphPad Prism 6 software). *$P < 0.05$ was considered significant for statistical tests.

Ethics

Animal experimentation: All mouse work was carried out following the recommendations from the National Research Council Guide for the Care and Use of Laboratory Animals, with the protocols approved by the Institutional Animal Care and Use Committee of Shanghai, China [SYXK (SH) 2011-0112]. All surgery was performed under sodium pentobarbital anesthesia, and every effort was made to minimize suffering.

Data availability

The authors declare that all data supporting the findings of this study are available within the article and its Supplementary Information files or are available from the authors upon request.

Supplementary Figures and Legends
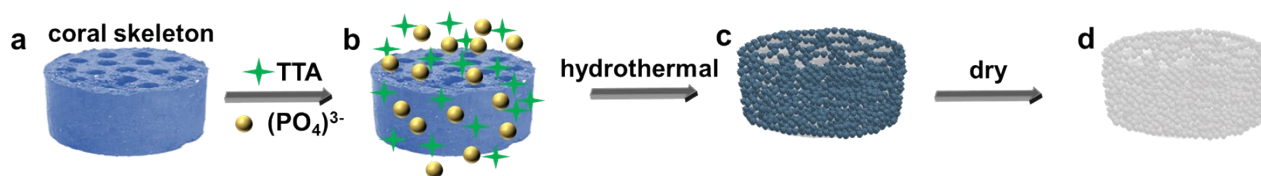
Figure S1. Schematic drawing of the synthetic process of CMHAP@CL scaffolds.

The porous blue coral stone was selected as the matrix skeleton and calcium source, and the chiral small molecule (TTA) was used as the inducer of symmetry breaking. Under the condition of hydrothermal synthesis, the coral stone decomposed and released Ca^{2+}, and then Ca^{2+} and the carboxyl group of tartrate molecule acted on each other through complexation. With the further progress of the reaction, $(PO_4)^{3-}$ gradually replaced the tartrate ion. Then, hydroxyapatite films are further assembled to form chiral mesoscopic structures and grown in situ on the coral stone frame. Finally, the chiral organic molecules are removed by sufficient rinsing and extraction to obtain CMHAP@CL scaffolds.
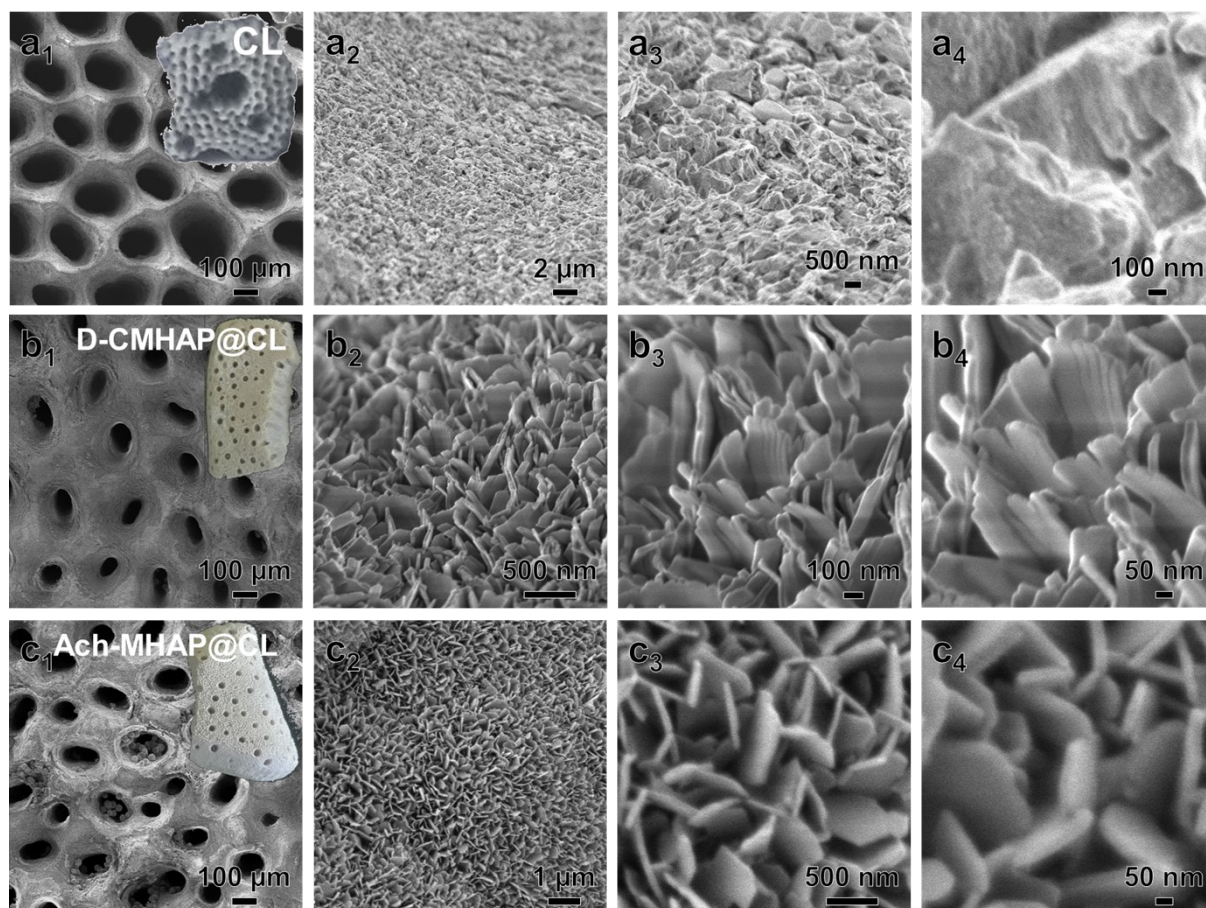
Figure S2. SEM images of CL(a) and D-CMHAP@CL(b) and Ach-MHAP@CL scaffolds(c).

Figure S2 shows SEM results of D-CMHAP@CL scaffolds and Ach-MHAP@CL generated under D-TTA and chiral molecule conditions. It was observed that the pore size was reduced, and the scaffolds formed on the surface of hydroxyapatite were scaffolds with lacerated scaffolds similar to those of left-handed molecular systems, with the opposite direction of spiral arrangement to L-CMHAP@CL scaffolds. However, a closer look shows that the Ach-MHAP@CL sheet formed by the chiral molecular system is slightly thinner and wider, with smooth edges and no tearing phenomenon. This suggests that the existence of chiral molecules is the key factor leading to the formation of chiral structures.
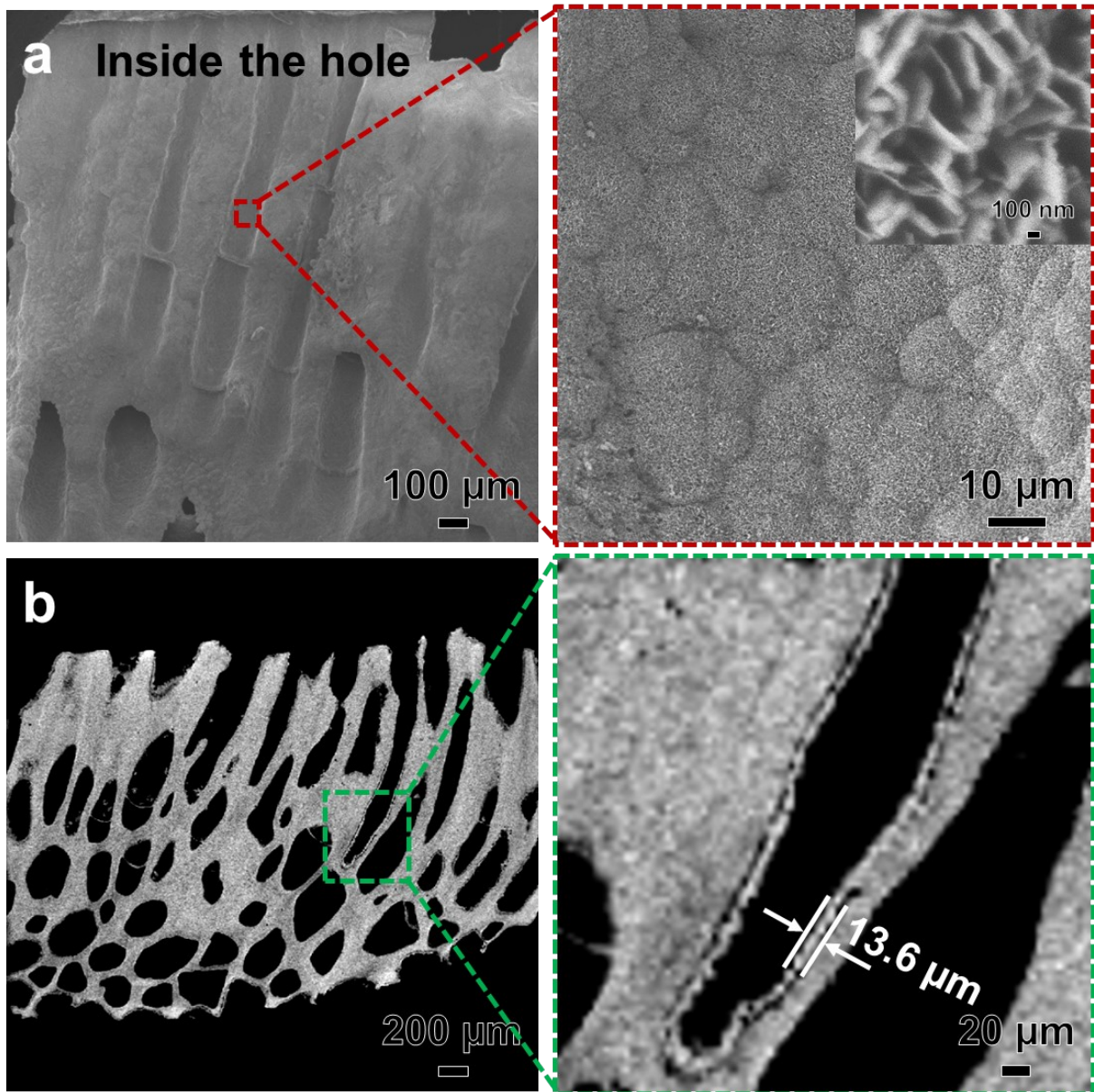
Figure S3. SEM images (a) and three dimensional CT images (b) of L-CMHAP@CL scaffolds.

As shown in Figure S3a, the section shows that the internal vertical channels are covered with sheet hydroxyapatite films, and the growth direction is perpendicular to the growth surface, which proves that this method can make the displacement reaction in the channels well and obtain three-dimensional scaffolds with full coverage of the internal and external surfaces of the pores. Figure S3b shows the 3D CT reconstructed and sectional morphologic features of L-CMHAP@CL scaffolds, further demonstrating that a layer of hydroxyapatite is formed on the coral stone with a thickness of ~ 13.6μm.
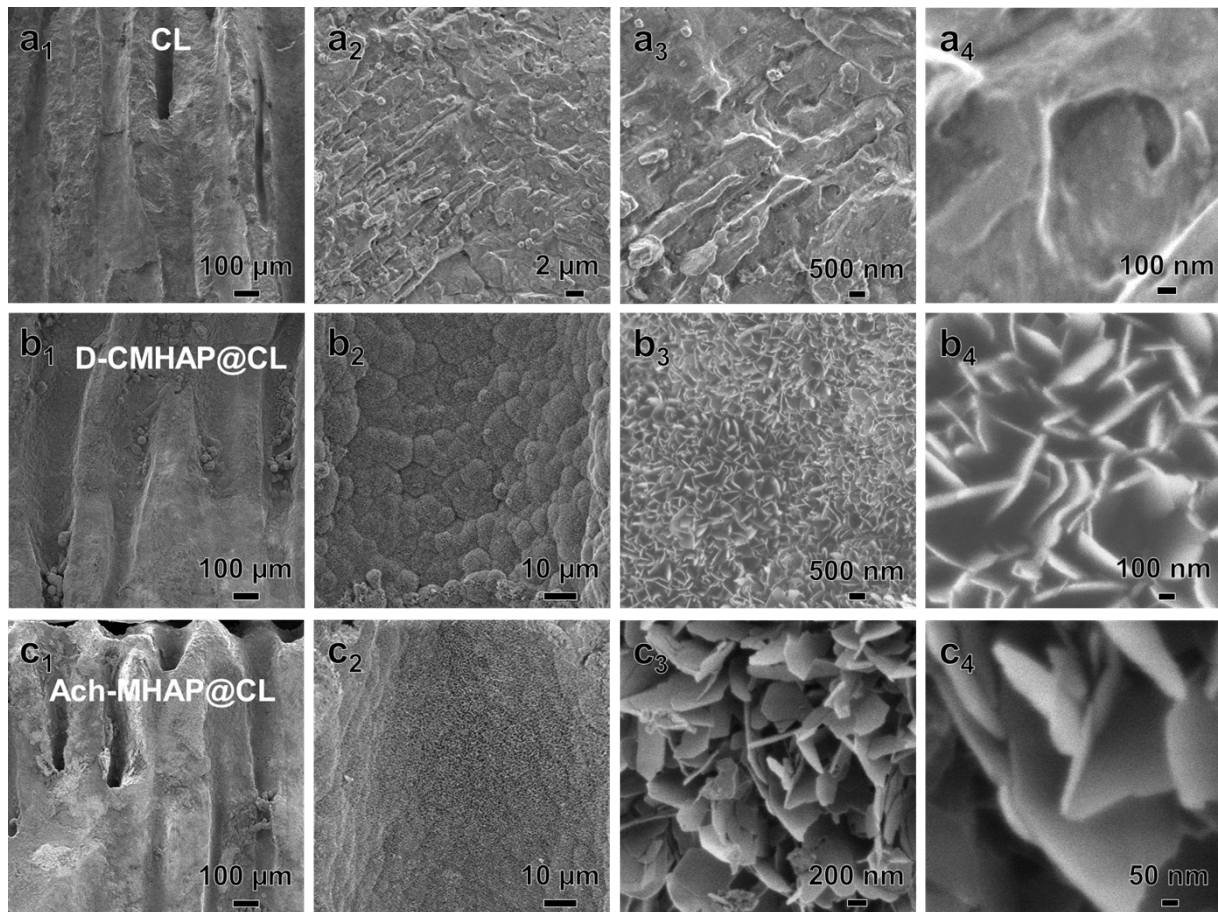
Figure S4. SEM images of coral (CL) (a) and D-CMHAP@CL (b) and Ach-MHAP@CL scaffolds (c) .

Figure S4 shows the SEM results of D-CMHAP@CL scaffolds and Ach-MHAP@CL sections generated under D-TTA and chiral molecules. It was found that the pore size of hydroxyapatite was reduced, and the scaffolds formed on the surface were scaffolds of lamellar structures. D-CMHAP@CL scaffolds induced by D-TTA were similar to L-CMHAP@CL scaffolds induced by L-TTA molecules, with torn scaffolds. However, the edges of the sheets of hydroxyapatite formed by the chiral molecular system are smooth and there is no tearing. It is consistent with the structure of HAP sheet formed on the surface of the scaffold.
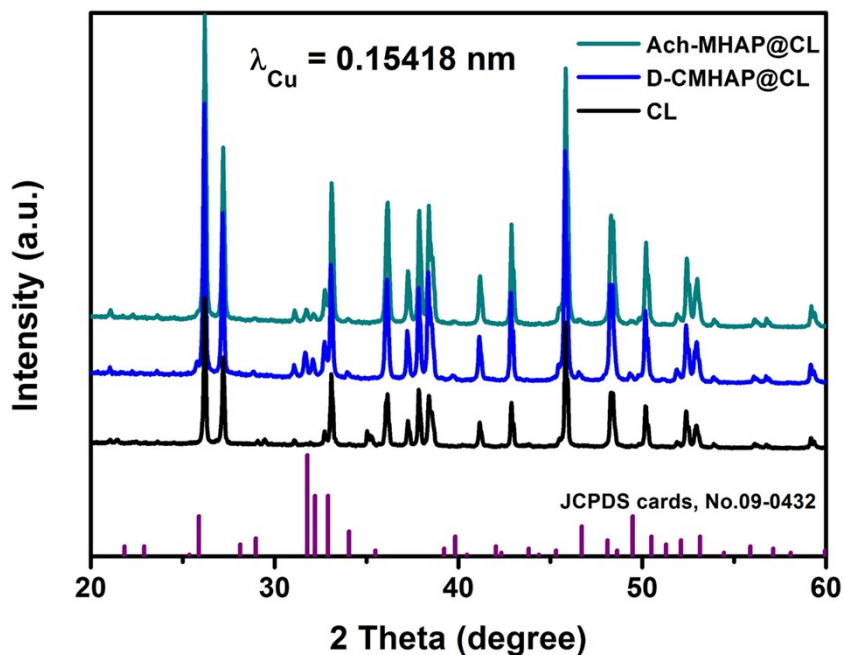
Figure S5. XRD patterns of CL and D-CMHAP@CL scaffolds and Ach-MHAP@CL scaffolds.

X-ray powder diffraction tests were also conducted on D-CMHAP@CL scaffolds and AchMHAP@CL right, as shown in Figure S5. The results were the same as those on L-CMHAP@CL scaffolds, with weak characteristic peaks of hydroxyapatite due to high content of calcium carbonate in the base. However, the characteristic peaks of HAP can still be clearly identified.
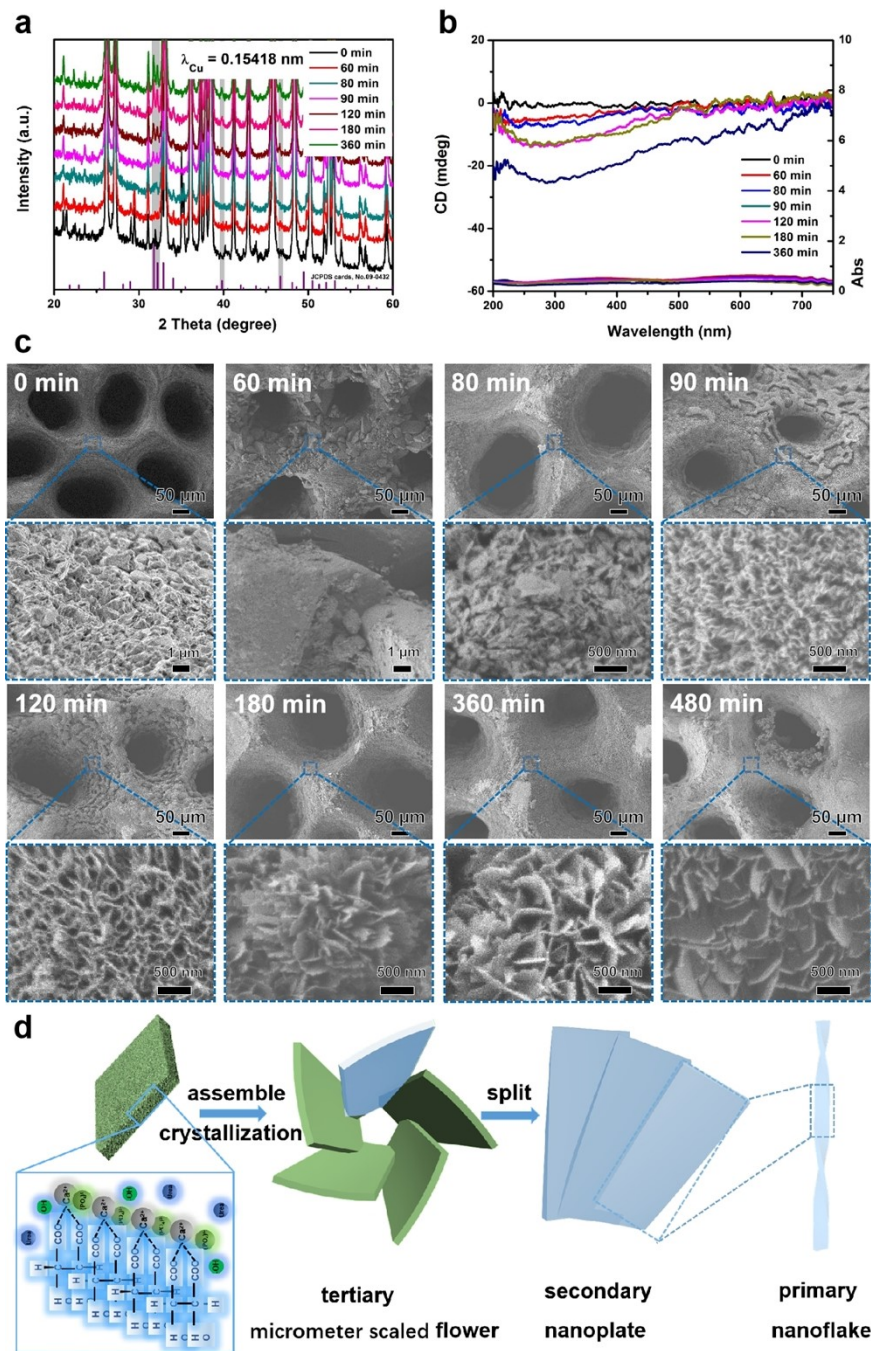
Figure S6. XRD (a) and DRCD and DRUV-Vis spectra (b) of CMHAP@CL scaffolds synthesized with different reaction time. SEM images (c) of CMHAP@CL scaffolds synthesized with different reaction time. Schematic diagram of formation mechanism of assembly structure (d) of CMHAP.

The chiral primary structure with a left-handed distorted crystal lattice would be induced by L-TTA, in which the carboxyl groups chelated well with the calcium ions, released during CL hydrothermal process. After mixing with phosphate ions and urea under heating, the phosphate ions displaced tartrate ions to form calcium phosphate precipitates. During reaction, the chiral arrangement of TTA molecules induced the oriented malposed growth of nanocrystals, thus leading to the formation of tertiary chiral spiral arrangement of twisted nanoplates. As induced by the continuous twisting of the crystal lattice, the secondary twisted nanoplate (Fig. S6) could not maintain as a whole single crystal over a large distance due to the distortion of the crystal lattice, which split into several primary nanoflakes.
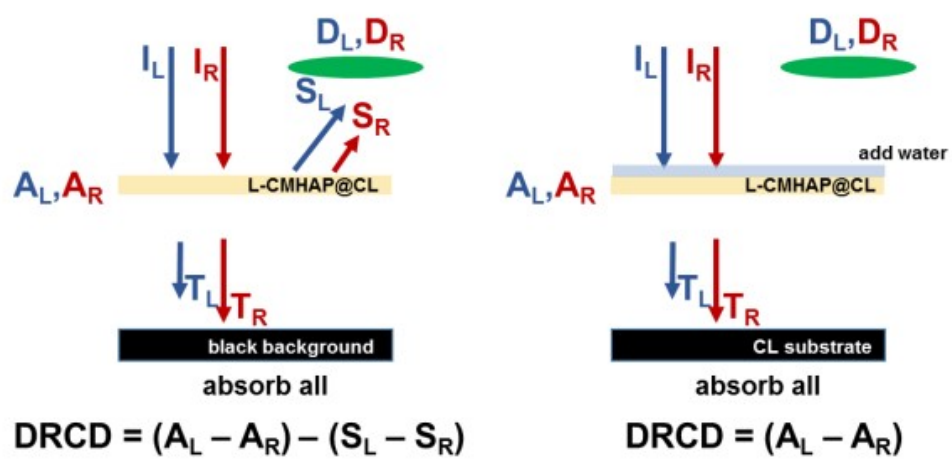
Figure S7. DRCD detection mechanism.
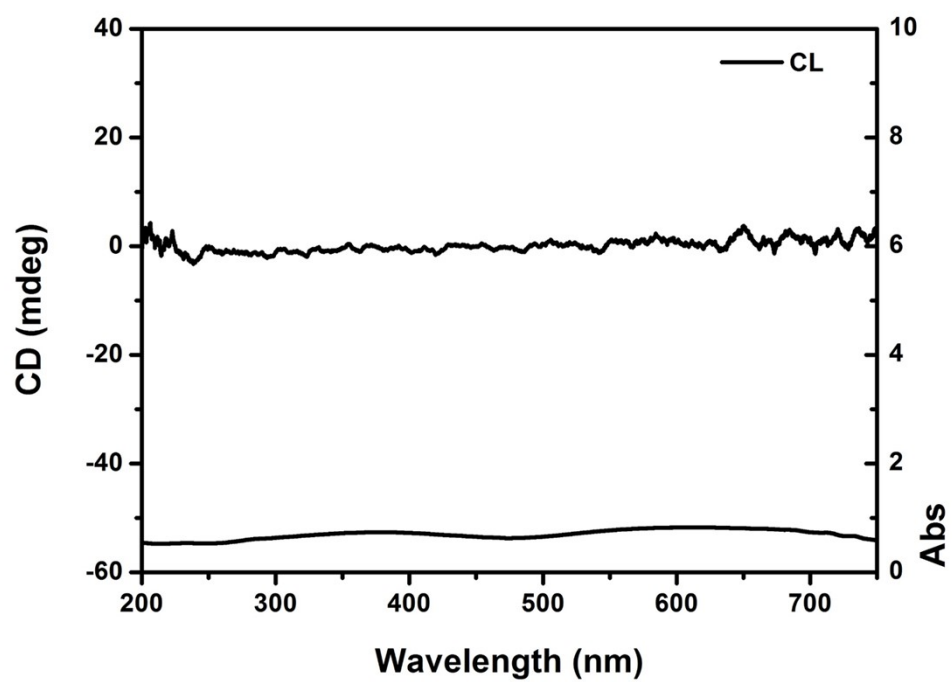
Figure S8. DRCD and DRUV-Vis spectrum of CL.
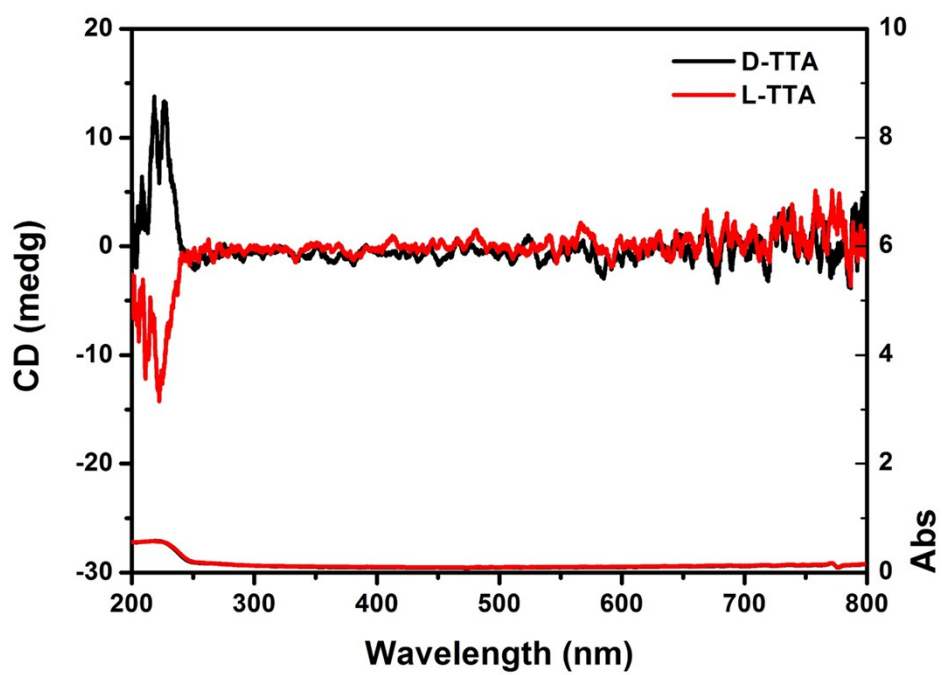
Figure S9. DRCD and DRUV-Vis spectrum of TTA.
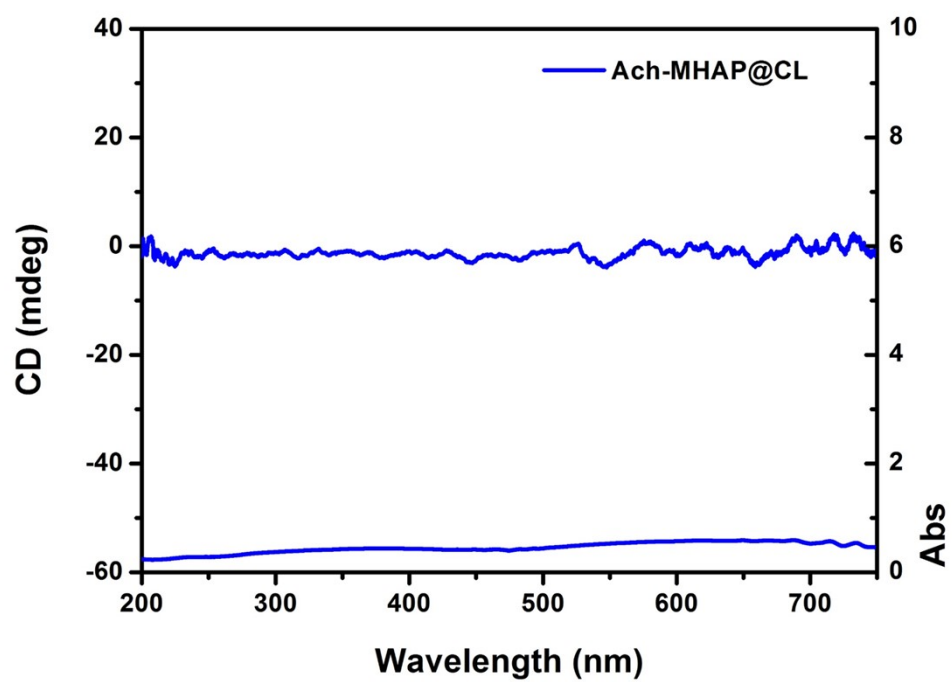
Figure S10. DRCD and DRUV-Vis spectrum of Ach-MHAP@CL scaffolds.
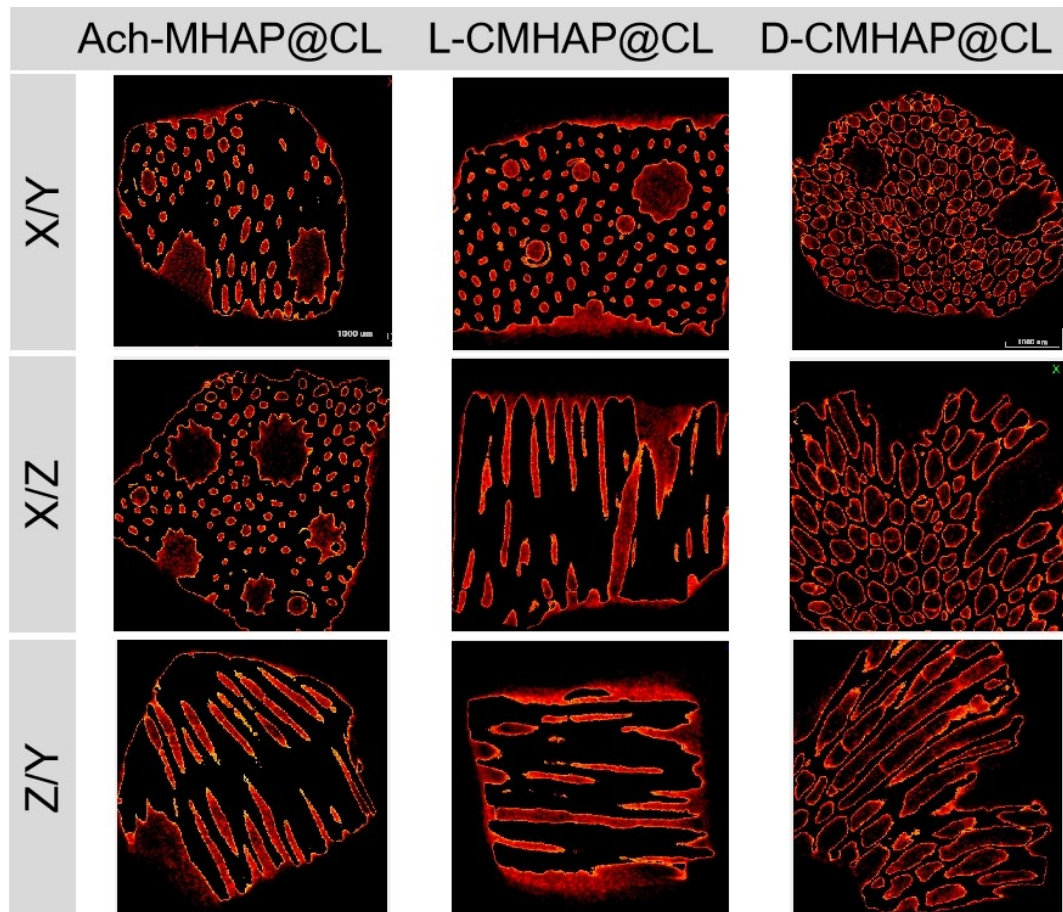
Figure S11. Three dimensional sectional section CT images of CL and CMHAP@CL scaffolds after 24 weeks implantation.
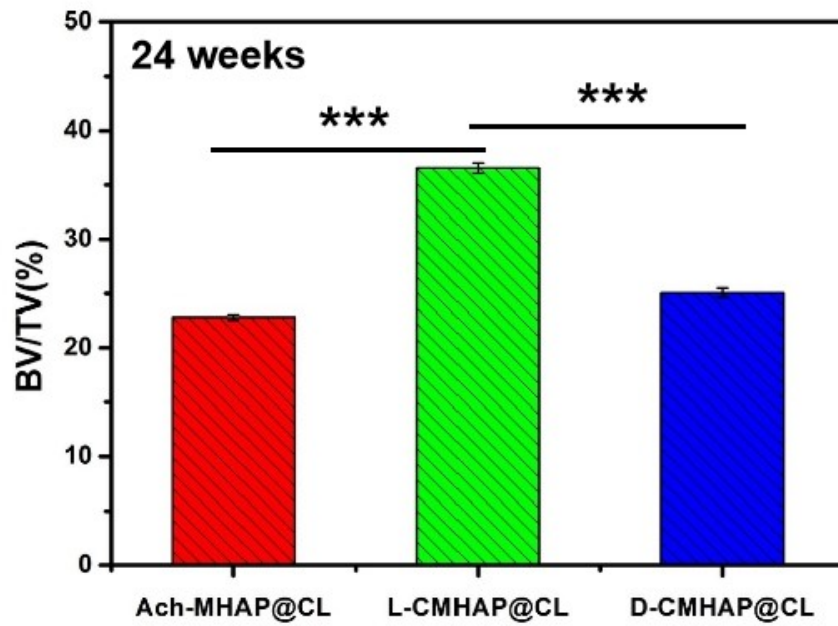
Figure S12. Quantitative analysis of the relative ratio of osteogenic volume of CMHAP@CL scaffolds in vivo after 24 weeks implantation.
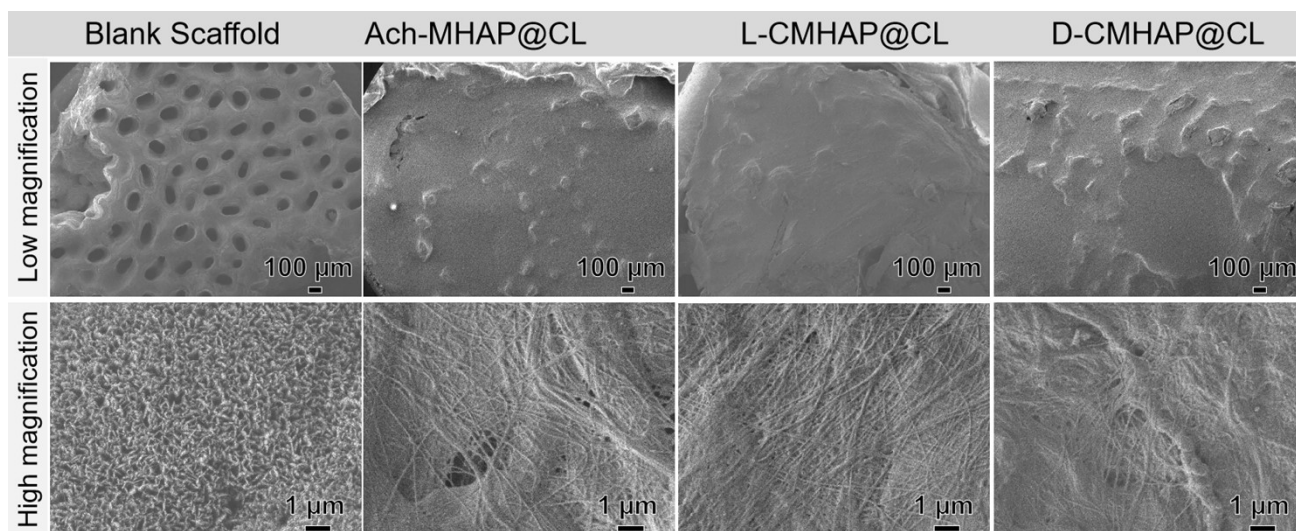
Figure S13. SEM images of the osteogenic of CMHAP@CL scaffolds in vivo.
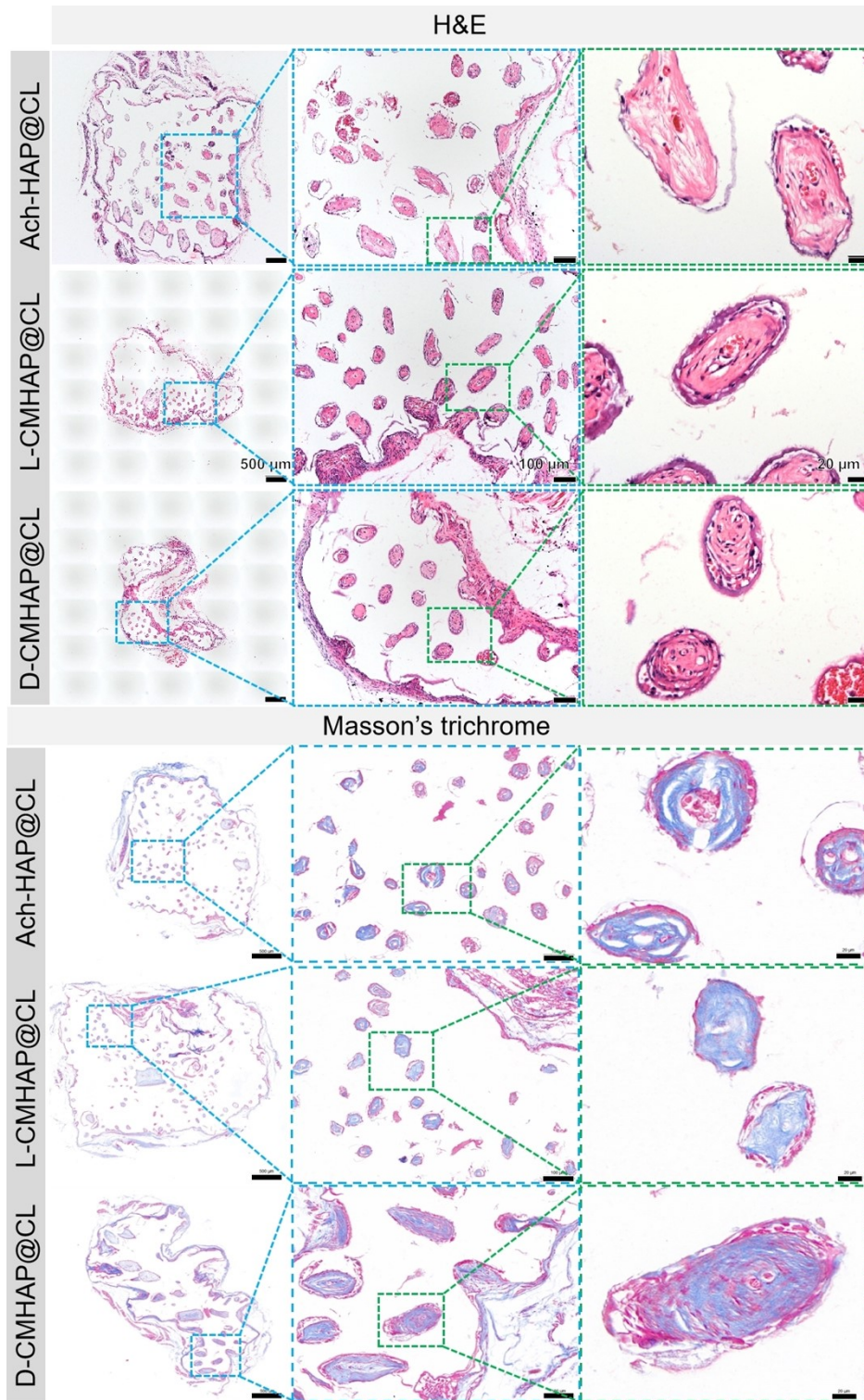
Figure S14. H&E and Masson's trichrome staining of osteogenesis 24 weeks in vivo of CMHAP@CL scaffolds, scale bar are 500, 100, 20 μm.
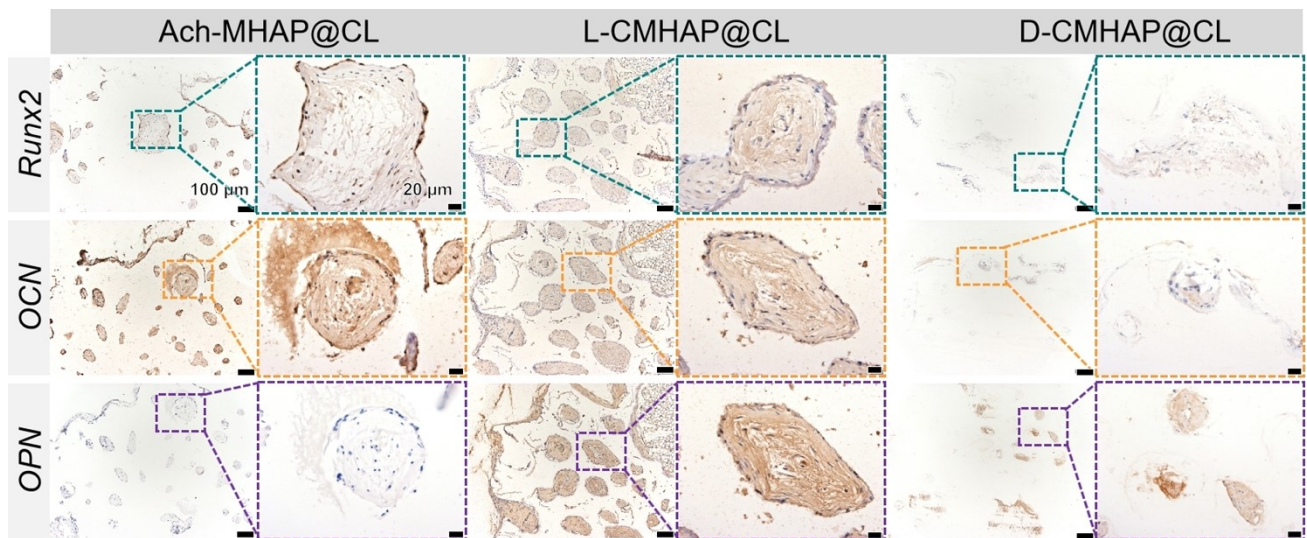
Figure S15. Immunohistochemical of osteogenic 24 weeks in vivo of CMHAP@CL scaffolds, scale bar are 100, 20 µm.